2004 International Symposium on Nonlinear
Theory and its Applications (NOLTA2004)
Fukuoka, Japan, Nov. 29 - Dec. 3, 2004

Experimental-Based Approach for Macromodel Synthesis of Interconnects

Junji KAWATA†, Yuichi TANJI‡, Yoshifumi NISHIO††,
Tomoji YOSHIDA†, Tetsuo TADA† and Akio USHIDA†

†Faculty of Engineering, Tokushima Bunri University
1314-1 Shido, Sanuki-shi, Kagawa 769-2193 Japan
‡Faculty of Engineering, Kagawa University
††Faculty of Engineering, Tokushima University
Email: {kawata,yoshida,tada,ushida}@fe.bunri-u.ac.jp, tanji@eng.kagawa-u.ac.jp, nishio@ee.tokushima-u.ac.jp

Abstract—In this paper, each element of the admittance matrix of RLCG interconnects is reduced by partial fraction consists of the exact poles of the admittance matrix and the corresponding residues. The residues can be calculated by the least squares method so that the partial fraction matches each element of the exact admittance matrix in the frequency-domain. From the partial fraction, macromodels which can be easily simulated with SPICE are synthesized. Based on experimental studies, an approach for calculating the residues that guarantee the passivity of the macromodels are presented.

1. Introduction

The analysis and design of high speed LSI chips are becoming more and more important, because the subcircuits coupled with interconnects embedded in the substrate sometimes cause the fault switching operations due to the signal delays, crosstalks, reflections and so on [1]-[5]. The Elmore resistance-capacitance (RC) delay metric is popular due to its simple closed-form expression, computation speed and fidelity with respect to the simulation [4]. The closed-form combining with the delay and crosstalk is firstly presented in the reference [5]. The modified algorithms are proposed later for the improvement of the accuracy and the practical applications in the simulations [6]-[9].

AWE (asymptotic waveform evaluation method) [10] is widely used as a reduction technique of the large scale of linear networks, the algorithm is based on a moment-matching technique and Padé approximation. However, the method sometimes become erroneous, if there exist the poles far from the origin. To overcome the problem, CFH (complex frequency hopping) [11] and multi-point Padé approximation [12] methods are proposed. In these reduction algorithms, the reduced circuits sometimes become unstable in the time domain even if all the poles are located in the left hand side of the complex plane. The ill-condition can be overcome by PVL (Padé via Lanczos process) [13], and PRIMA (passive reduced-order interconnect macromodeling algorithm) [2,14]. In order to apply these algorithms to the interconnects, we need two steps such that each interconnect is firstly modeled by a finite order system, and Arnoldi-based congruence transformation is applied to the system to form its reduced order model.

In this paper, we consider LSIs such as ASIC or SoC (System on a Chip) are coupled with interconnects embedded in the substrate. In this case, the diffusion resistance components of the interconnects are generally assumed to be very large compared to those of PCBs [3] and the lengths are very short. From the telegrapher's equation of the interconnects, the admittance matrix is derived from the relations at the near and far ends [1]. Next, each of the elements of the admittance matrix is approximated by partial fraction using dominant poles around the origin. The poles can be calculated by a computational method proposed in our previous study [18]. The residues are subsequently evaluated by the least squares method so that the frequency response curves of the partial fractions match with those of the exact admittance matrix. Here the frequency response curves of the partial fractions are compared with the exact ones. Then, it will be investigated that how the passivity of partial fractions obtained from pole-residue pairs breaks and why inaccurate residues are obtained. Based on the considerations, we provide a procedure to enforce the passivity of the macromodels.Furthermore, SPICE simulations using the macromodel synthesized from the partial fractions and built-in model of SPICE are carried out and compared.

2. Admittance Matrix of Interconnects and Partial Fraction Approximation

The admittance matrix for a uniform N coupled RLCG interconnect is given by [18]:

$$\left.\begin{aligned} \mathbf{Y}_{11}(s) = \mathbf{Y}_{22}(s) &= \mathbf{P}_c(s)\mathrm{diag}[\coth\gamma_i(s)d]\mathbf{P}_v(s)^{-1} \\ \mathbf{Y}_{12}(s) = \mathbf{Y}_{21}(s) &= -\mathbf{P}_c(s)\mathrm{diag}\left[\frac{1}{\sinh\gamma_i(s)d}\right]\mathbf{P}_v(s)^{-1} \end{aligned}\right\} \quad (1)$$

where $P_v(s)$ and $P_c(s)$ are transfer matrices. The poles of the admittance matrix (1) must satisfy the relation $\sinh\gamma_i(s)d = 0$ and they can be calculated by applying the Leverrier-Faddeeva algorithm [18]. We choose some dominant poles located around the origin of the complex plane, because the poles have large impact on the transient responses. Thus, the admittance matrix given by (1) are approximated by the partial fractions that are composed of the dominant poles and the corresponding residues, in the following form:

$$\hat{Y}_{11}(s) = \hat{Y}_{22}(s) = \sum_{i=1}^{N} \frac{k_{01,i}}{s - p_{0,i}} + \sum_{i=1}^{N}\sum_{n=1}^{M} \frac{b_{11,i,n}s + b_{10,i,n}}{s^2 + a_{1,i,n}s + a_{0,i,n}} \quad (2)$$

$$\hat{Y}_{12}(s) = \hat{Y}_{21}(s) = \sum_{i=1}^{N} \frac{k_{02,i}}{s - p_{0,i}} + \sum_{i=1}^{N}\sum_{n=1}^{M} \frac{b_{21,i,n}s + b_{20,i,n}}{s^2 + a_{1,i,n}s + a_{0,i,n}} \quad (3)$$

where N is the number of conductors and M shows the number of complex conjugate pairs. Also $p_{0,i}$ denotes a real pole and $\{a_{1,i,n},\ a_{0,i,n}\}$ are derived from complex conjugate poles for (1), respectively. Further the residues of (2) and (3) have the following relations [17, 18]:

$$\left.\begin{array}{l} k_{02,i} = -k_{01,i} \\ b_{21,i,n} = (-1)^{n+1} b_{11,i,n},\ \ b_{20,i,n} = (-1)^{n+1} b_{10,i,n} \end{array}\right\} \quad (4)$$

that is, we have to evaluate only the residues for (2) and the values of (3) can be calculated using the relation (4). Macromodels can be derived from the relations (2)–(4), but omit in this paper due to space limitation (refer to [18] for detail).

3. Approach for Calculating Residues

The residues satisfying (2) are calculated by the least squares method so that the frequency response curve of (2) fits to the exact one. In order to guarantee the passivity of the macromodels, the following trial-and-error approach for calculating the residues is provided.

Step 1) Determine the highest matched frequency f_{max}.

Step 2) Choose all poles with the imaginary part less than or equal to $2\pi f_{max}$ and further several extra poles beyond the frequency. Let the number of the former and the latter be M and α, respectively. Thus the number of poles required in the least squares method is replaced with $M_{ext} = M + \alpha$. The appropriate initial value of α is about $5 \sim 10$.

Step 3) Perform the least squares fitting and subsequently truncate the extra α pole-residue pairs beyond $2\pi f_{max}$.

Step 4) If all of the residues and the resulting macromodel parameters are positive, finish the computation; otherwise increase the number of extra poles α and return to Step 3.

It should be noted that the proposed approach enforces the passivity of the interconnect macromodels. All the values of the passive elements included in the macromodels are constrained to be positive. Hence, the macromodels are guaranteed to be passive.

We mention here the reason why the above residues calculation procedure is required, through the following numerical results.

Case 1 Let the highest frequency and the number of poles be $f_{max} = 6$ [GHz] and $M = 10$, respectively. In this case the frequency corresponding to the pole p_{10} (the suffix $i = 1$ is omitted) with largest imaginary part is about 5 [GHz]. The frequency response curve obtained by substituting the calculated poles and residues to the partial fraction (2) or (3) and the exact curve obtained from (1) are shown in Fig. 1. Here, the above-mentioned procedure of residues calculation is not used, and $|\hat{Y}_{12}(j\omega)|$ is calculated using the relation (4). The approximated curves by the partial fractions have relatively good agreement with the exact one up to 11-th peak around 5 [GHz], because we took a real pole and 10 of complex conjugate poles (i.e., $M = 10$). From the figure, it seems that the least squares fitting is successfully performed. However the calculated residues contain negative values as listed in the left-half of table 1, which yields negative circuit parameters. Thus, it is clear that the passivity is not satisfied in this case.

Case 2 For the case that the resistance component of interconnect becomes large, the least squares fitting fails to approximate the frequency-domain response accurately, as shown in Fig. 2. In this example, $|\hat{Y}_{12}(j\omega)|$ is also calculated using the relation (4). From these two examples, we can conclude that the pole selection in this manner is not suitable for our purpose.

Case 3 Next we tried to choose some extra poles beyond the highest frequency f_{max}. After choosing 6 of extra poles beyond $f_{max} = 6$ [GHz] (i.e., $M = 18$), the residues are calculated by performing the least squares fitting, which are listed in the right-half of table 1 and the frequency response curves are shown in Fig. 3. As expected, $|\hat{Y}_{11}(j\omega)|$ matches the exact one within the whole frequency range

Table 1: Residues obtained by the least squares method for Cases 1 and 3.

	Case 1		Case 3	
n	$b_{1,n}$	$b_{0,n}$	$b_{1,n}$	$b_{0,n}$
1	3.815e−02	3.979e−03	4.000e−02	5.002e−03
2	3.815e−02	1.939e−03	4.000e−02	5.008e−03
3	3.816e−02	−1.568e−03	4.000e−02	5.017e−03
4	3.818e−02	−6.727e−03	4.000e−02	5.016e−03
5	3.820e−02	−1.385e−02	4.000e−02	5.004e−03
6	3.822e−02	−2.349e−02	4.000e−02	4.979e−03
7	3.825e−02	−3.664e−02	4.000e−02	4.940e−03
8	3.828e−02	−5.537e−02	4.000e−02	4.960e−03
9	3.829e−02	−8.508e−02	4.000e−02	5.049e−03
10	3.818e−02	−1.483e−01	4.000e−02	5.127e−03
11			4.000e−02	4.623e−03
12			3.990e−02	1.383e−02
13			4.149e−02	3.551e+00
14			1.704e+00	−1.005e+02
15			−1.902e+01	6.750e+02
16			6.859e+01	−1.764e+03
17			−9.761e+01	1.972e+03
18			4.815e+01	−7.910e+02

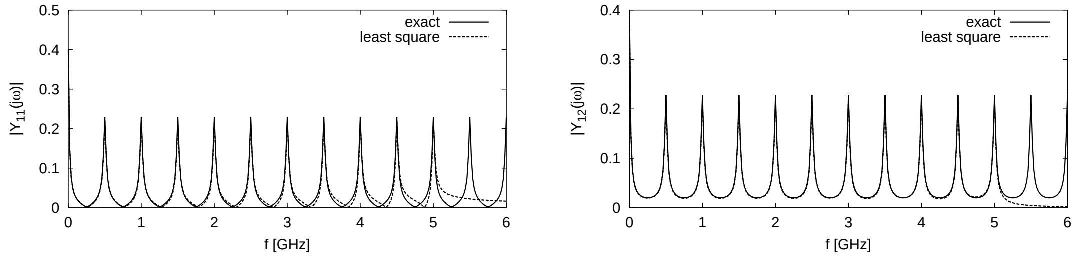

(a) $|Y_{11}(j\omega)|$ (b) $|Y_{12}(j\omega)|$

Figure 1: Frequency response curves for single conductor interconnect. ($r = 0.5[\Omega/\text{mm}]$, $d = 5.0[\text{mm}]$, $f_{max} = 6.0[\text{GHz}]$, $M = 10$)

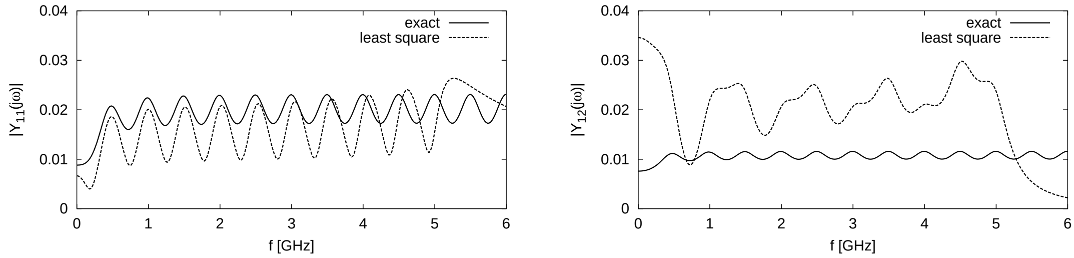

(a) $|Y_{11}(j\omega)|$ (b) $|Y_{12}(j\omega)|$

Figure 2: Frequency response curves for single conductor interconnect. ($r = \mathbf{25.0}[\Omega/\text{mm}]$, $d = 5.0[\text{mm}]$, $f_{max} = 6.0[\text{GHz}]$, $M = 10$)

($0 \le f \le f_{max}$) of interest, shown in Fig. 3(a). Unfortunately, as shown in Fig. 3(b), $|\hat{Y}_{12}(j\omega)|$ obtained from (3) and (4) is entirely different from the exact one. Furthermore, the values of $|\hat{Y}_{11}(j\omega)|$ at certain frequency range beyond the highest matched frequency ($f_{max} = 6$ [GHz]) become very large and differ completely from the exact one, as shown in Fig. 3(c). Note that the only difference of Figs. 3 (a) and (c) is the scales of axes.

From the right-half of table 1, the residues for $n > 12$, which correspond to the extra poles, contain negative or large values and consequently do not guarantee the passivity. Thus, it is concluded that disagreement of $|\hat{Y}_{12}(j\omega)|$ and huge values of $|\hat{Y}_{11}(j\omega)|$ at frequency range beyond f_{max} are due to the extra pole-residue pairs.

Case 4 In this example, to remove the pole-residue pairs beyond the highest frequency, which are the factors disturbing our purpose, is considered. In the same conditions as Case 3, 6 of extra pole-residue pairs for $n > 12$ are truncated and the frequency response curves are computed. The results are illustrated in Fig. 4. The effect of truncation begins to appear at the last half of the frequency range; that is, the accuracy of partial fractions (2) and (3) at higher frequency range is degraded. However, at lower frequency range both curves remain matched. Further the calculated response $|\hat{Y}_{12}(j\omega)|$ using the relation (4) is also matched to the exact one at lower frequency range, unlike the Case 3. Note that the partial fractions (2) and (3) (or the resulting asymptotic equivalent circuits) become more precise as the value of f_{max} increases, because matched frequency range becomes wide accordingly. Further it has been confirmed that positive residues and/or circuit elements of the macromodels can be obtained by increasing the number of extra poles, even if negative residues and/or circuit elements appeared around f_{max}.

It is not easy to show whether the residues guaranteeing the passivity can be always obtained by this approach, however they could be obtained in our simulations conducted so far.

4. Transient Simulation Using Macromodels

The transient responses for a simple linear circuit with a single-conductor interconnect are calculated. The SPICE simulations using the macromodel are carried out with varying the highest matched frequency f_{max} (accordingly M is changed), and compared with the simulated results of built-in SPICE model. Figure 5 shows the transient response waveforms for $r = 0.5$ [Ω/mm] and $d = 5.0$ [mm]. All the waveforms have relatively good agreement, although ringing occurs at rising and falling edges of waveforms. The ringing can be suppressed with increasing M, but remarkable changes are not observed even for $M = 100$ (in this case $f_{max} = 50$ [GHz]).

5. Conclusions

In this paper, we have provided an approach for calculating the residues that guarantee the passivity. Using the exact poles and the calculated residues, each element of the admittance matrix of interconnects is approximated by the partial fraction. Though the frequency response curves calculated using the partial fractions become inaccurate around the highest matched frequency f_{max}, the partial fractions and the resulting macromodels are always passive. In this paper, some examples for single conductor interconnect have been presented, but our method can be effectively applied to multi-conductors interconnects.

References

[1] J. A. Brandao Faria, *Multiconductor Transmission-Line Structures: Modal Analysis Techniques*, John Wiley and Sons, Inc., 1993.

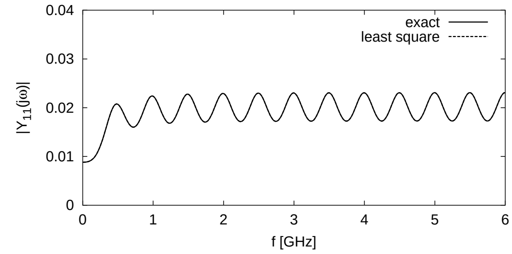

(a) $|Y_{11}(j\omega)|$

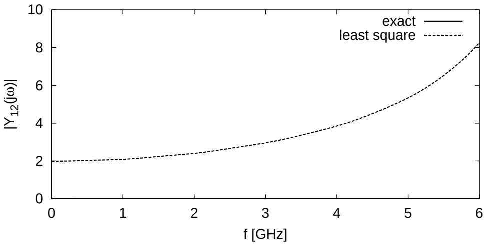

(b) $|Y_{12}(j\omega)|$

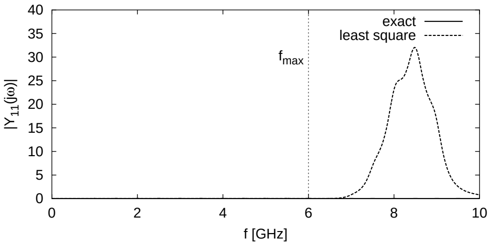

(c) $|Y_{11}(j\omega)|$

Figure 3: Frequency response curves for the case that extra poles beyond f_{max} are used. (r = **25.0**[Ω/mm], d = 5.0[mm], f_{max} = 6.0[GHz], M = 18)

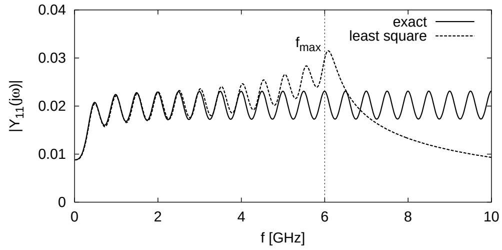

(a) $|Y_{11}(j\omega)|$

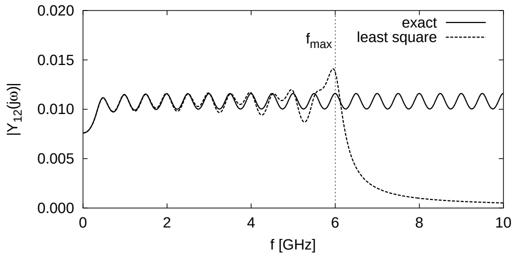

(b) $|Y_{12}(j\omega)|$

Figure 4: Frequency response curves for the case that 6 poles beyond f_{max} are truncated. (r = **25.0**[Ω/mm], d = 5.0[mm], f_{max} = 6.0[GHz], M = 12, α = 6)

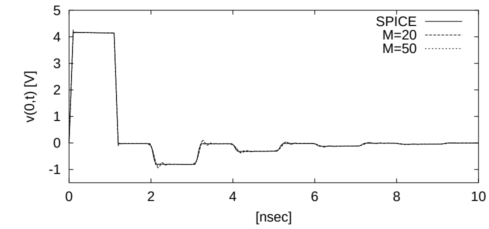

(a) near end.

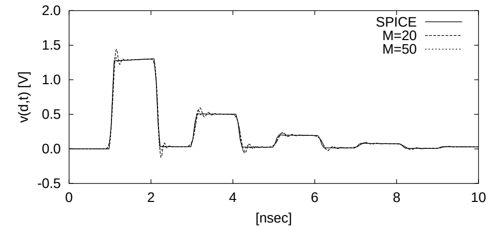

(b) far end.

Figure 5: Transient responses of example circuit. (r = 0.5 [Ω/mm], d = 5.0 [mm])

[2] M. Celik, L. Pileggi and A. Odabasioglu, *IC Interconnect Analysis*, Kluwer Academic Pub., 2002.

[3] J. L. Wyatt, Jr.,“Signal propagation delay in RC models for interconnect,” *Circuit Analysis, Simulation and Design*, A. E. Ruehli(Editor), Elsevier Science Pub. B.V.(North-Holland), pp. 254–291, 1987.

[4] W. C. Elmore, “The transient response of damped linear networks with particular regard to wideband amplifiers,” *J. Appl. Phys.*, vol. 19, pp. 55–63, Jan. 1948.

[5] T. Sakurai, “Closed-form expressions for interconnection delay, coupling, and crosstalk in VLSI’s,” *IEEE Trans. Electron Devices*, vol. 40, pp. 118–124, 1991.

[6] S-Y. Kim, N. Gopal and L. T. Pillage, “Time-domain macromodels for VLSI interconnect analysis,” *IEEE Trans. Computer-Aided Design*, vol. 13, pp. 1257–1270, 1994.

[7] R. Gupta, B. Tutuianu and L. T. Pileggi, “The Elmore delay as a bound for RC trees with generalized input signals,” *IEEE Trans. Computer-Aided Design*, vol. 16, pp. 95–104, 1997.

[8] C. J. Alpert, A. Devgan and C. V. Kashap, “RC delay metrics for performance optimization,” *IEEE Trans. Computer-Aided Design*, vol. 20, pp. 571–582, 2001.

[9] T. Kimura and M. Okumura, “An efficient reduction method of a substrate RC network model,” *IEICE Trans. Fundamentals*, vol. E84-A, pp. 698–704, 2001.

[10] E. Chiprout and M. S. Nakhla, *Asymptotic Waveform Evaluation and Moment Matching for Interconnect Analysis*, Kluwer Academic Pub., 1994.

[11] E. Chiprout and M. S. Nakhla, “ Analysis of interconnect networks using complex frequency hopping(CHF),” *IEEE Trans. Computer Aided Design*, vol. CAD-14, pp. 186–200, 1995.

[12] Q. Yu, J. Meiling and E. S. Kuh, “Passive multipoint moment matching model order reduction algorithm on multiport distributed interconnect networks,” *IEEE Trans. Circuits and Systems-I*, vol. 46, pp. 140–160, 1999.

[13] P. Feldmann and R. W. Freund, “Efficient linear analysis by Padé approximation via the Lanczos process,” *IEEE Trans. Computer Aided Design*, vol. CAD-14, pp. 639–649, 1995.

[14] A. Odabasioglu, M. Celik and L. T. Pileggi, “PRIMA: Passive reduced-order interconnect macromodeling algorithm,” *IEEE Trans. Computer Aided Design*, vol. 17, pp. 645–654, 1998.

[15] A. Ushida, K. Urabe, Y. Yamagami and Y. Nishio, “Asymptotic equivalent circuits of interconnects based on complex frequency method,” *ECCTD’01*, vol. 3, pp.29–32, 2001.

[16] D. K. Faddeeva and V. N. Faddeeva *Computational Methods of Linear Algebra*, W. H. Freeman and Co., 1963.

[17] Y. Yamagami, Y. Nishio, A. Hattori and A. Ushida, n“A reduction technique of large scale RCG interconnects in complex frequency domain,” *ISCAS’03*, vol. 3, pp.490–493, 2003.

[18] J. Kawata, Y. Tanji, Y. Nishio and A. Ushida, “Asymptotic equivalent circuits of interconnects and the passivity,” *Tech. Rep. of IEICE*, no.NLP2003-134, pp.43–48, 2003.